



Article

Minimalist Design for Multi-Dimensional Pressure-Sensing and Feedback Glove with Variable Perception Communication

Hao Ling ¹, Jie Li ², Chuanxin Guo ², Yuntian Wang ², Tao Chen ^{1,2,*} and Minglu Zhu ^{1,*}

¹ Jiangsu Provincial Key Laboratory of Advanced Robotics, School of Mechanical and Electric Engineering, Soochow University, Suzhou 215123, China; 20224229012@stu.suda.edu.cn

² School of Future Science and Engineering, Soochow University, Suzhou 215123, China; 2262405057@stu.suda.edu.cn (J.L.); 2262405007@stu.suda.edu.cn (C.G.); 2262405004@stu.suda.edu.cn (Y.W.)

* Correspondence: chent@suda.edu.cn (T.C.); mlzhu@suda.edu.cn (M.Z.)

Abstract: Immersive human–machine interaction relies on comprehensive sensing and feedback systems, which enable transmission of multiple pieces of information. However, the integration of increasing numbers of feedback actuators and sensors causes a severe issue in terms of system complexity. In this work, we propose a pressure-sensing and feedback glove that enables multi-dimensional pressure sensing and feedback with a minimalist design of the functional units. The proposed glove consists of modular strain and pressure sensors based on films of liquid metal microchannels and coin vibrators. Strain sensors located at the finger joints can simultaneously project the bending motion of the individual joint into the virtual space or robotic hand. For subsequent tactile interactions, the design of two symmetrically distributed pressure sensors and vibrators at the fingertips possesses capabilities for multi-directional pressure sensing and feedback by evaluating the relationship of the signal variations between two sensors and tuning the feedback intensities of two vibrators. Consequently, both dynamic and static multi-dimensional pressure communication can be realized, and the vibrational actuation can be monitored by a liquid-metal-based sensor via a triboelectric sensing mechanism. A demonstration of object interaction indicates that the proposed glove can effectively detect dynamic force in varied directions at the fingertip while offering the reconstruction of a similar perception via the haptic feedback function. This device introduces an approach that adopts a minimalist design to achieve a multi-functional system, and it can benefit commercial applications in a more cost-effective way.

Keywords: haptic feedback; piezoresistive sensor; pressure sensing; wearable HMI; liquid metal; motion capture



Citation: Ling, H.; Li, J.; Guo, C.; Wang, Y.; Chen, T.; Zhu, M. Minimalist Design for Multi-Dimensional Pressure-Sensing and Feedback Glove with Variable Perception Communication. *Actuators* **2024**, *13*, 454. <https://doi.org/10.3390/act13110454>

Academic Editor: Samer Mohammed

Received: 8 October 2024

Revised: 7 November 2024

Accepted: 10 November 2024

Published: 13 November 2024



Copyright: © 2024 by the authors. Licensee MDPI, Basel, Switzerland. This article is an open access article distributed under the terms and conditions of the Creative Commons Attribution (CC BY) license (<https://creativecommons.org/licenses/by/4.0/>).

1. Introduction

With the rapid development of human–machine interaction technology, wearable devices capable of providing precise motion capture, pressure sensing and feedback are becoming increasingly important [1–3]. These devices show great potential in areas such as virtual reality (VR) [4,5], medical rehabilitation [6–8], and robotic control [9–12]. The advancement of the human–machine interface (HMI) relies heavily on the simulation and reproduction of the human body’s complex sensory systems [13], including vision [14,15], hearing [16], and touch [17,18]. Among these, the introduction of tactile information significantly enhances the immersion and sense of presence in the user’s interaction process, thereby improving the overall interactive experience [19]. However, current wearable HMIs still face many challenges in multi-dimensional haptic information sensing and feedback [20,21], and the integration of more and more feedback actuators and sensors can lead to serious problems such as large and complex systems [22,23].

Existing wearable HMIs often struggle to simultaneously sense multi-dimensional pressure and hand motion when faced with complex hand movements [24,25]. For

example, many flexible sensors can only sense a single dimension of dynamic or static pressure and lack appropriate feedback actuation methods to effectively support multi-dimensional feedback [26–29]. For users, systems lacking comprehensive feedback mechanisms may result in unnatural interactions, even affecting the user experience and the practical application of the system [30]. Therefore, the development of a multi-dimensional haptic sensory feedback HMI with a simple structure and a high degree of integration is of great research significance and application value [31].

To address this challenge, this paper proposes a glove that enables multi-dimensional pressure sensing and feedback with a minimalist design for the functional units. The as-fabricated device uses PDMS (polydimethylsiloxane) as a substrate, with encapsulated liquid metal microchannels designed to construct both piezoresistive pressure sensors (Figure 1(i)) and bending sensors (Figure 1(iii)). The haptic feedback function is enabled by coin vibrators (Figure 1(ii)), while the vibrational feedback can be monitored through triboelectric signals via a liquid-metal-based sensing unit. The modular design of the liquid metal microchannel films allows the detection of pressure and bending signals during various interactions. To realize multi-dimensional pressure sensing and the corresponding perception regeneration, two pressure sensors and feedback vibrators are symmetrically distributed at the fingertip. By collaboratively evaluating the relationship between two sensing signals, the direction and dynamic features of pressure information can be extracted. Similarly, the actuation intensities of two vibrators can be individually tuned to mimic the varied directions of mechanical stimulus in real time. Hence, this approach shows the possibility of using minimal functional units to achieve more functions via specific design and data analysis, as well as programming. In summary, this study proposes a facile design for a wearable HMI glove that integrates multi-dimensional dynamic and static pressure sensing, bending detection of individual joints, and multi-dimensional haptic feedback, providing new insights and methods regarding a cost-effective, simple, and multi-functional solution for more user-friendly HMI technologies. Specifically, the main contributions include the following. (1) A minimalist design for a structure with a multi-modal human–machine interface is proposed, which is realized by the simplified distribution of sensors and actuators for multi-directional pressure sensing and haptic feedback. (2) The symmetrical distribution of two pressure sensors and two coin vibrators on each fingertip makes it possible to detect and generate dynamic and static pressure from different directions, and it is immune from the size variation issue of hands caused by different users. (3) The pressure and bending sensors, which share the same fabrication process, enable low-cost production and maintenance. Meanwhile, the output signals of these sensors are easily processed, thereby enhancing the efficiency of human–machine interaction and enabling the accurate sensing of pressure and hand posture. The following sections of this paper will detail the sensor design principles, system integration methods, and experimental validation results, and discuss the potential applications in HMIs.

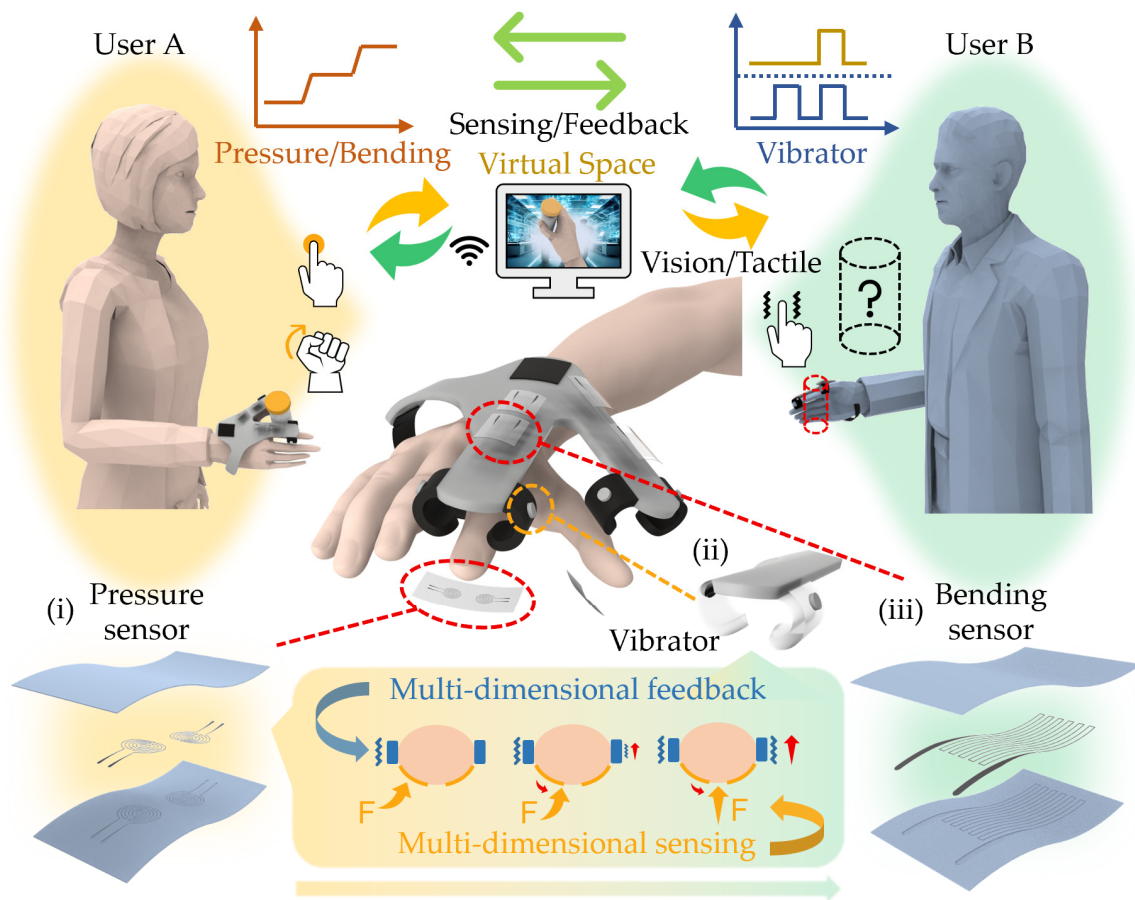


Figure 1. Multi-dimensional pressure-sensing and feedback glove and its intelligent interaction system. Schematic diagram of the glove's application in enhanced spatial immersive interaction, including (i) the structural diagram of the pressure sensor, (ii) the components of the vibration haptic feedback module, and (iii) the structural diagram of the bending sensor.

2. Materials and Methods

2.1. Design and Sensing Mechanism of the Sensing and Feedback Glove

The sensing modules use liquid metal as the conductive layer and PDMS (polydimethylsiloxane) as the elastic substrate, relying primarily on the embedded liquid metal microchannels within the PDMS film to detect external force signals [32]. As shown in Figure 2a, the pressure sensor is designed with a circular microchannel structure [33], with three loops around an area of approximately 7 mm^2 . The cross-sectional dimensions of the microchannel are about $80 \text{ }\mu\text{m}$ wide and $50 \text{ }\mu\text{m}$ high, and the spacing between each loop is 0.4 mm . As shown in Figure 2b, for the joint bending-sensing unit, a reciprocating grid design is used [34], with twelve liquid metal microchannels, each 20 mm long, evenly distributed along the finger's direction. The spacing between each microchannel is 0.8 mm , and the cross-sectional dimensions are $120 \text{ }\mu\text{m}$ wide and $50 \text{ }\mu\text{m}$ high. Both sensing units share a similar structural design, with the overall thickness of the flexible sensor based on the PDMS film being approximately $400 \text{ }\mu\text{m}$.

In terms of the interactive glove, as shown in Figure 2c, the pressure-sensing units are placed symmetrically on the thumb and index fingertips in a horizontal arrangement. This layout allows the pressure-sensing units on both sides to independently detect forces from different directions applied to the sides of the fingers. Additionally, they can work together to sense pressure in the middle of the index finger, enabling the detection of off-center pressures by analyzing the signal magnitude difference between the two sides. Furthermore, a pair of coin vibrators are placed symmetrically on both sides of the flexible

pressure-sensing units to act as feedback actuators. At a rated voltage and load, the coin vibrator, made of aluminum alloy (7 mm in diameter and 2 mm in thickness), has an operating frequency of 150 Hz and an amplitude of 0.3 g. Each coin vibrator corresponds to the pressure-sensing unit on the same side. When a pressure signal is detected on the interactive glove worn by user A, the corresponding coin vibrator on user B's glove will generate haptic feedback. The larger the pressure signal, the greater the power applied to the coin vibrator, resulting in a higher vibration frequency and more pronounced feedback. Through this mechanism, the interactive glove provides the user with multi-dimensional information, such as the magnitude and direction of the pressure applied to the fingertip, enhancing the human-machine interaction experience.

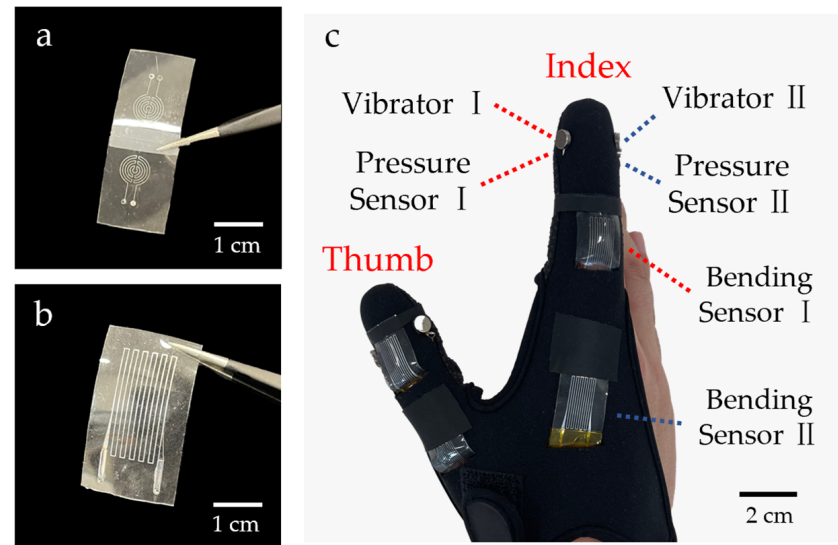


Figure 2. Sensors of the multi-dimensional pressure-sensing and feedback glove. (a) Optical image of the pressure sensor; (b) optical image of the bending sensor; and (c) optical image of the interactive glove and the corresponding components.

Additionally, joint bending-sensing units are placed at the two main bending joints of each finger [35]. By analyzing the signals from these two units, the system can accurately estimate the bending state of the user's fingers. By further integrating the signals from multiple finger-joint bending-sensing units, it is possible to reconstruct the hand posture in a virtual space [36]. Through visual information, users can monitor the joint positions of the interactive object's hand in real time [37]. In Figure 2c, each sensor and feedback device is labeled for distinction.

Both sensing units are based on piezoresistive sensing mechanisms. When the flexible sensing unit is stimulated by external force, the electrical resistance of the microchannels increases due to their reduced cross-sectional areas, increased channel lengths, or both [38]. By monitoring this change, we can detect pressure information and the bending movement of the finger joints [39]. The difference lies in the fact that, as shown in Figure 3a, for the pressure sensor, the primary cause of the resistance change is the reduction in the cross-sectional area of the liquid metal microchannel when pressure is applied. For the bending sensor, as shown in Figure 3b, the primary cause of the resistance change is the elongation of the liquid metal microchannel when the sensor is stretched due to finger bending.

It should be clarified that the bending-sensing unit refers to a sensor that is able to measure the bending of the joint in hand, which is essentially a strain sensor. When the finger is bending, both sides of the sensing unit fixed on the glove will generate strain due to the change in the distance between the fixed points after bending, and the sensor itself does not respond to curvature changes.

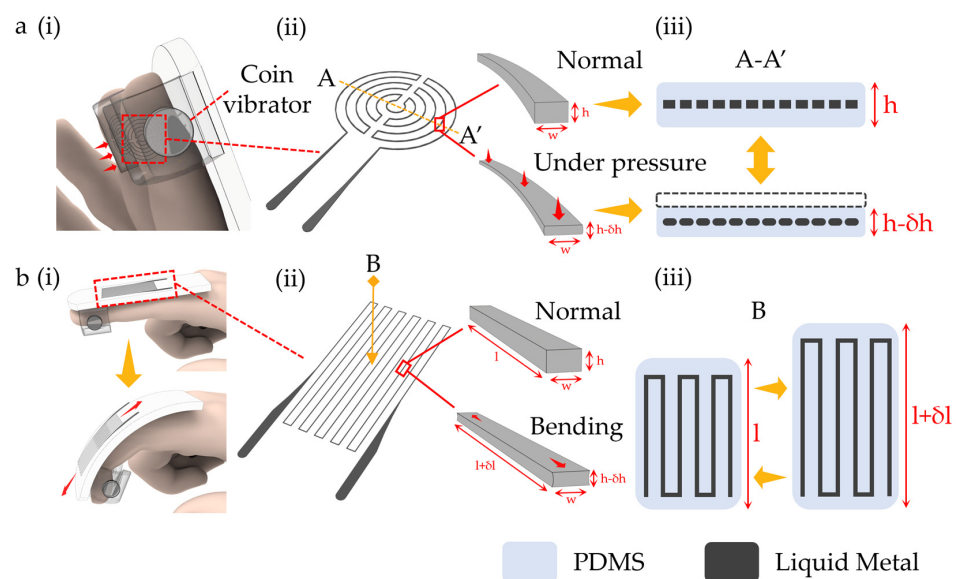


Figure 3. Working mechanism of the pressure sensor and the bending sensor. (a) The (i) schematic diagram of the pressure sensor, (ii) dimensional changes of the liquid metal electrodes in the normal and pressurized states, and (iii) changes in the A-A' cross-section of the liquid metal electrodes; and (b) the (i) schematic diagram of the bending sensor, (ii) changes in the liquid metal electrodes in the normal and bending states, and (iii) dimensional changes in the bending sensors observed from view B.

2.2. Preparation of Flexible Sensors

The pressure-sensing unit and bending-sensing unit are fabricated using the same process. Both consist of liquid metal electrodes, elastic PDMS films, and wires. The detailed preparation steps are as follows [40].

(1) Preparation of Microchannel Molds

First, glass slides ($6\text{ cm} \times 5\text{ cm}$) are cleaned three times with acetone and alcohol, followed by 3 min of ultrasonic cleaning. The glass surface is then dried with nitrogen gas and placed on a $120\text{ }^{\circ}\text{C}$ hotplate for 20 min to evaporate any remaining moisture, ensuring the glass surface is completely dry. A DuPont photosensitive dry film, approximately the same size as the glass, is cut, with one side of its protective film removed. The film is then applied to the glass moistened with water and pressed tightly using a laminator. After removing the protective film from the other side, a photosensitive layer with a thickness of approximately $40\text{ }\mu\text{m}$ is obtained. Next, the pattern of the flexible sensor is exposed to UV light using a mask for 6 s. The exposed pattern forms the required microchannels, while the unexposed areas are thoroughly cleaned with a 1.5% sodium carbonate solution. The surface is then rinsed with deionized water to remove any remaining sodium carbonate solution, dried with nitrogen, and baked at $50\text{ }^{\circ}\text{C}$ for 30 min.

(2) Fabrication of Flexible Sensors

To facilitate the easy release of the PDMS elastomer from the mold, $10\text{ }\mu\text{L}$ of dimethylchlorosilane is applied to the mold surface, which is then placed in a vacuum environment for 10 min, allowing the volatilized silane to settle on the glass surface. Dow Corning Sylgard 184 Silicone Elastomer Clear is mixed at a 10:1 ratio to prepare the liquid PDMS. The liquid PDMS is degassed in a vacuum desiccator for 30 min to remove any air bubbles. It is then spin-coated onto the microchannel mold at 400 rpm for 20 s, forming a PDMS film embedded with microchannels, with a thickness of approximately $230\text{ }\mu\text{m}$. The PDMS film is cured at $70\text{ }^{\circ}\text{C}$ for 1 h. During this step, a hole punch is used to create an injection port in the microchannel film. Another layer of PDMS film is made similarly, but the liquid PDMS is spin-coated at 600 rpm for 20 s on a plain glass surface, forming a film approximately $140\text{ }\mu\text{m}$ thick after curing. The PDMS

film with microchannels and the plain PDMS film are both exposed to oxygen plasma at 150 W for 120 s. The two films are then bonded together and baked at 70 °C for 30 min to create a permanent bond. Finally, liquid metal is carefully injected into the microchannels using a syringe, and Sil-Poxy silicone adhesive is used to seal the inlet and outlet with external connecting wires.

2.3. Assembly of the Sensing Feedback Glove

First, a Velcro and strap design is used to insert the pressure sensor devices into the thumb and index fingertips [41]. After that, it is ensured that they are securely fixed by adjusting the tightness of the straps, with the wires routed closely along the inside of the glove to the wrist. Next, four coin vibrators should be attached with adhesive to the appropriate position on either side of the glove's fingertips. A small hole is then made in the back of the glove, allowing the wires from the pressure-sensing units to pass through to the wrist along the same path. Finally, the bending-sensing units are installed at the main joints of the thumb and index finger, with two sensors per finger. The tops of the sensing units are fixed to the glove using black adhesive tape, while the bottoms are inserted into pre-made holes in the glove and also secured with black adhesive tape. The wire bundles are routed closely along the inside of the glove to the wrist. After marking all the wire bundles, they are organized and housed in a soft tube, ultimately connecting to their respective sensing signal acquisition and feedback drive circuits [42].

According to the working mechanism of the bending sensor, placing the sensor on the top of the finger can bring out its performance to the fullest. On the other hand, compared with the bottom and sides of the finger, the upper part is least likely to be affected by external forces when in contact with an object. Hence, this installation method for the bending-sensing unit can also reduce unnecessary measurement errors.

2.4. Control System of Sensing and Feedback

The Arduino MEGA 2560 (Arduino S.r.l., Monza, Italy) is used as the microprocessor for the sensing and feedback circuits. In the sensing section, both types of sensing units read signals by capturing the voltage changes between them and the voltage divider resistors [43]; the pressure-sensing unit uses a 1 k Ω voltage divider resistor (Uni-royal, Kunshan, China), while the bending-sensing unit uses a 150 Ω voltage divider resistor (Uni-royal, Kunshan, China). Notably, for the pressure-sensing unit, the sensing signal requires additional preprocessing through an LM324 operational amplifier (CJ, Nanjing, China), with a gain of 21 times. The processed signal is then read via the digital I/O pins of the Arduino development board. For the feedback section, an external 5 V power supply drives the coin vibrators. To control the power supplied to the coin vibrators, the LH8050QLT1G transistor (LRC, Leshan, China) and LL4148 diode (ST, Dongguan, China) are used to program the PWM pins of the Arduino.

2.5. Characterization Methods of the Sensing Units

For the pressure-sensing unit, a force gauge (MultiTest 2.5-i, Mecmesin, Slinfold, UK) combined with a 3D-printed testing probe is used to cyclically apply and release pressure on the sensing unit, and the pressure values are measured via a commercial sensor (ILC 50N, Mecmesin, Slinfold, UK), as shown in Figure 4a. The contact size of the testing probe is the same as the area of the sensing unit [44–46]. For the bending-sensing unit, we fix both ends of the sensing unit using a clamp, securing it to the force gauge [47]. By controlling the relative displacement of the force gauge's elevating rod at a speed of 100 mm/min, we conduct a tensile test on the sensing unit, as shown in Figure 5a. During the test, the oscilloscope (MSO54B, Tektronix, Beaverton, OR, USA) measures the output voltage changes of the sensing circuit. Each test is repeated three times, and the average value is taken.

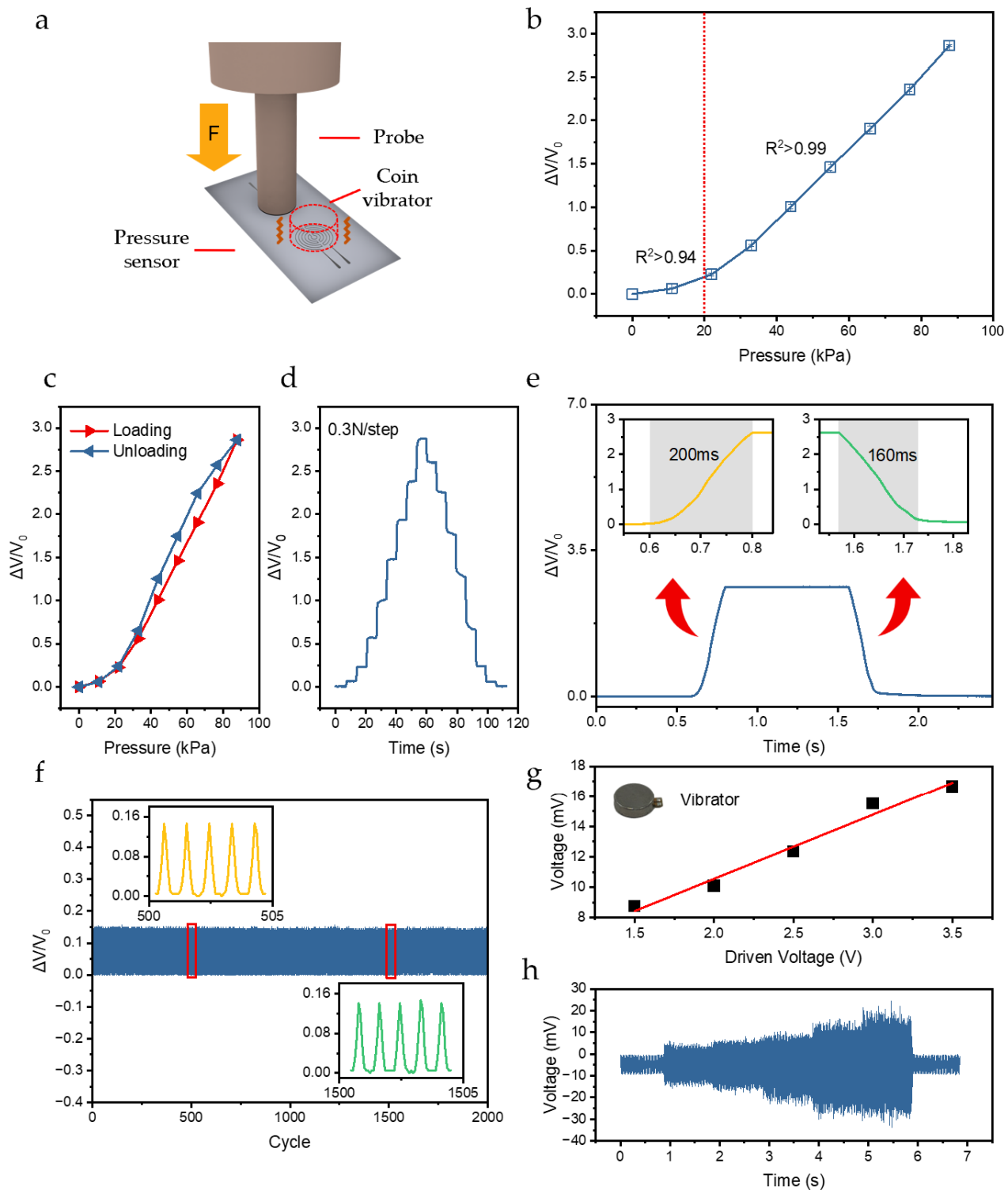


Figure 4. Characterization of the pressure sensor. (a) Schematic of the characterization method; (b) relationship between the sensor's output signal and the pressure under loading conditions; (c) relationship between the pressure sensor's output signal and the pressure under loading and unloading conditions; (d) real-time monitoring of the output signal changes during one cycle of pressure increase and decrease; (e) response and recovery times of the sensor; (f) repeatability test over 2000 cycles at 55 kPa; (g) relationship between the driven voltage of a coin vibration and the collected triboelectric voltage signal of the sensor; and (h) real-time triboelectric voltage signal as the driven voltage continues to increase.

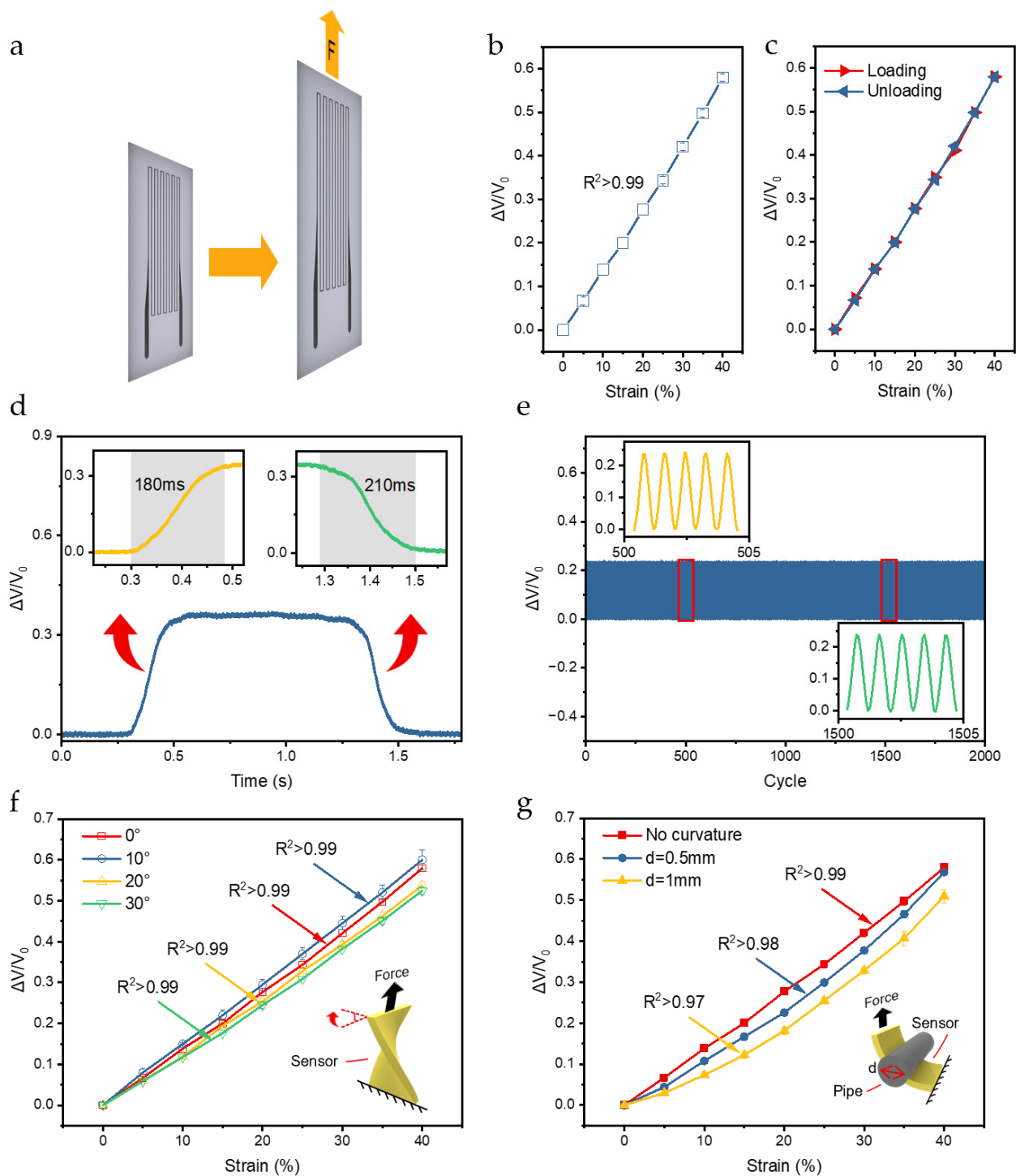


Figure 5. Characterization of the bending sensor. (a) Schematic of the characterization method; (b) relationship between the sensor's output signal and the strain under tensile conditions; (c) relationship between the bending sensor's output signal and the pressure under loading and unloading conditions; (d) response and recovery times of the sensor; (e) repeatability test over 2000 cycles at 20% strain; (f) response of the sensor to strain with a given initial torsion angle; and (g) response of the sensor to strain with a given initial curvature.

2.6. Characterization Methods of Vibration Feedback

Based on the principle of triboelectric sensing [48], the coin vibrators are then placed in close contact with the pressure-sensing unit, powered by a programmable power supply (UDP3305S, UNI-T, Dongguan, China) to drive them at different power levels. A position

comparison test at a rated voltage has been performed and is provided in Figure S1, indicating that the triboelectric signals can also be captured no matter where the coin vibrators are placed on the sensors. Simultaneously, an oscilloscope is used to read the output voltage of the sensing unit and record the average output voltage [49].

3. Results

3.1. Characterization of the Pressure-Sensing and the Vibration Feedback Units

To characterize the pressure-sensing units, a programmable force gauge and testing probe are used to apply static or dynamic pressure on the sensor surface, while a commercial sensor measures the applied force. Details of the experimental setup and methodology are described in Section 2. Figure 4b shows the average relationship between $\Delta V/V_0$ and pressure under the applied conditions, based on three measurements. Each point in the figure represents a record taken every 0.3 N (approximately 11 kPa) until the pressure reaches 2.4 N (approximately 88 kPa). This relationship curve is divided into two linear regions. In the range of 0–20 kPa, the sensitivity of the pressure-sensing unit is approximately 0.1032 kPa^{-1} , with linearity $R^2 > 0.94$. In the range of 20–100 kPa, the sensitivity is about 24.9773 kPa^{-1} , with linearity $R^2 > 0.99$. Considering the noise level of the sensor, the minimum detectable pressure is about 3.7 kPa. It is important to note that the reported detection limit is constrained by the measurement setup, and the true detection limit of the device may be lower. The error bars indicate one standard error. Due to the mechanical properties of the elastic materials, the sensing signal exhibits a certain hysteresis effect during unloading, as is shown in Figure 4c, with a percentage of 11.79%. However, when the force gradually unloads to 0 N, the output signal returns to the origin, indicating that the sensing unit can clearly and stably discern pressure changes of 0.3 N. Figure 4d shows a signal image from one cycle of real-time output voltage during three loading and unloading cycles. Figure 4e displays the response (200 ms) and recovery (160 ms) time of the pressure-sensing unit during loading/unloading, demonstrating its ability to respond instantaneously to external force stimuli. Additionally, the stability of the sensing unit is evaluated by cyclically loading/unloading a pressure of 55 kPa for 2000 cycles, as shown in Figure 4f. The experimental results indicate that the output signal of the pressure-sensing unit remains stable overall during the 2000 loading/unloading cycles. Five cycles of test data are extracted from the 500th and 1500th cycles, demonstrating the high perceptual stability and reproducibility of the sensing unit. Furthermore, additional tests are performed on the repeatability of the measurement accuracy of the pressure sensor, as can be seen in Figure S2a. The above experimental results indicate that the pressure sensor introduced in this work exhibits good sensing performance and can be widely applied in the field of human–machine interaction.

To calibrate the feedback intensity of the coin vibrators, based on the principle of triboelectric sensing, the pressure-sensing unit is employed for measurement. Details of the measurement method are described in Section 2. The measurement results are plotted in Figure 4g, showing an approximate linear relationship between the driving voltage, sensor output, and actual vibration amplitude, which can help provide adjustable vibration intensity in practical applications. Figure 4h demonstrates the real-time triboelectric signal of the pressure-sensing unit as the driving voltage increases, which also allows for real-time monitoring and calibration of the feedback intensity of the coin vibrators during interactions.

3.2. Characterization of the Bending-Sensing Unit

To characterize the bending-sensing unit, static or dynamic tensile forces are applied to the clamped sensing unit by adjusting the elevating rod of a programmable force gauge. The experimental setup and methodology details are described in Section 2. Figure 5b shows the average relationship between $\Delta V/V_0$ and the amount of extension during a stretch of up to 40%, based on three measurements. Each point in the figure represents a record taken every 5% of extension. In the 0–40% stretching range, the strain coefficient GF

of the bending-sensing unit is approximately 1.45, with linearity $R^2 > 0.99$. For the bending sensor, its loaded and unloaded outputs show good consistency, with a relatively small hysteresis percentage of 1.77% over its operating range (finger bending from 0° to 90°), which can be seen in Figure 5c. Figure 5d shows the response (180 ms) and recovery (210 ms) time of the bending-sensing unit during rapid loading/unloading, demonstrating its immediate responsiveness to external stimuli. In Figure 5e, it is demonstrated that the sensing unit can stably endure 2000 strain cycles, with five cycles of test data extracted from the 500th and 1500th cycles. Further repeatability experiments are performed in Figure S2b, proving the sensing unit's high robustness, which is crucial for flexible wearable sensing systems.

To assess the performance of the sensor in practical applications, the sensor is simulated being placed on a non-planar surface such as a finger, comparing the sensor's response to various initial torsion angles around its long axis (illustrated in Figure 5f). Similarly, the actual effects of bending under different curvatures are compared (illustrated in Figure 5g). The experimental results are presented in Figure 5f,g, indicating that in the torsion experiment, the sensor's response to tensile forces remains linear ($R^2 > 0.99$) even with the initial torsion angles; however, the sensor's sensitivity slightly decreases with an increasing torsion angle, approximately 0.3% per degree. In the curvature experiment, when the sensor experiences a certain bending curvature, its linear response remains good ($R^2 > 0.97$). As the curvature increases, its sensitivity also decreases to some extent. This change may result from the sensor not only experiencing the tensile stress applied by the force gauge but also a certain pressure exerted by the cylindrical object, causing the sensor to bend during testing. Overall, the sensing unit proposed in this paper demonstrates stable and reliable performance across various complex scenarios in practical applications.

3.3. Application of Multi-Dimensional Sensing and Augmented Haptic Feedback

In practical applications, the performance tests of pressure sensing are conducted by integrating the sensors into a glove to verify their capability for sensing multi-dimensional pressure, and additional tests of the system's overall delays for processing the signals have been performed and are detailed in Text S1, Figures S3 and S4 in the Supplementary File. Figure 6a shows the sensing tests performed on the left side (i), right side (ii), center (iii), and dynamic rotation from left to right (iv) of the right index fingertip, with the results displayed in Figure 6b. The results indicate that the pressure-sensing unit, once integrated into the glove, can effectively sense static or dynamic forces from different directions and dimensions.

Additionally, based on the principle of time-multiplexed sensing feedback, the real-time feedback capability of the coin vibrators is tested again. Figure 6c illustrates the vibration feedback signals collected based on the triboelectric sensing mechanism as the fingertip rotates from left to right on an object. When Sensor I on the left side of the fingertip first detects pressure, coin-vibrator I starts operating and gradually increases the feedback intensity to the corresponding level. Subsequently, when the fingertip reaches the center position, coin-vibrator II also activates. When the fingertip rotates to the right side, coin-vibrator I stops working due to the lack of pressure on the Sensor I side, while coin-vibrator II continues to vibrate until pressure from Sensor II disappears as the fingertip leaves the object.

Similarly, a single bending sensor is integrated into the glove, corresponding to the middle joint of the index finger, to validate its practical application. Figure 6d shows the sensor signals as the index finger joint bends from a straight position to 90° . During testing, our volunteer paused every 10° . The results demonstrate that the bending sensor can relatively accurately detect the bending state of the human finger. It is important to note that the reported detection accuracy is limited by the experimental setup, and the actual detection accuracy of the device may be higher. In Figure 6e, the impacts of different bending methods on the sensor performance are compared. The results indicate that regardless of how the user wearing the glove bends their fingers—whether in terms of

speed or method—the detection of the sensor is unaffected. Additionally, information on the bending speed can be extracted from the slope of the signal curve, achieving a more comprehensive sensing of bending actions.

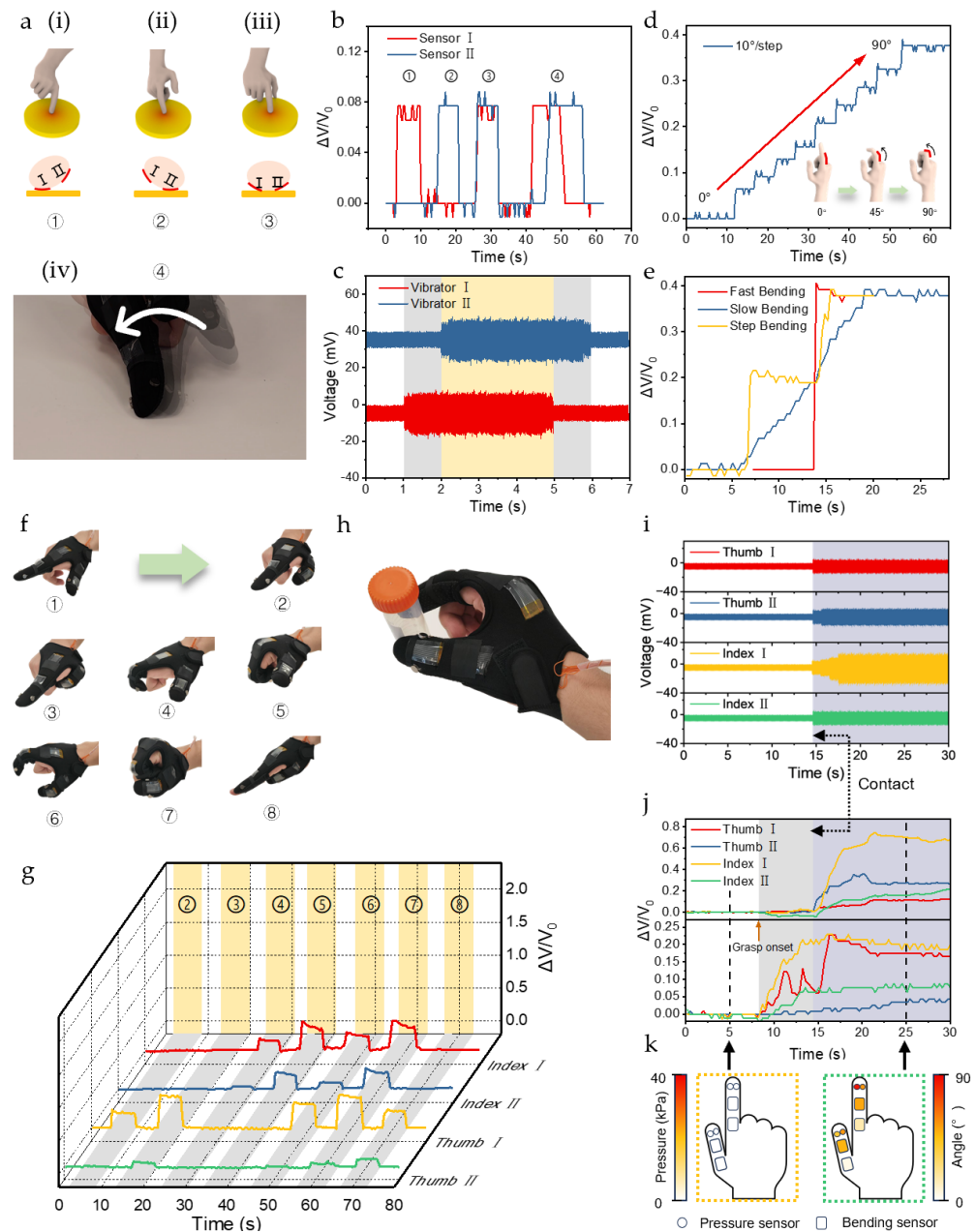


Figure 6. Demonstration application of the multi-dimensional pressure-sensing and feedback glove. (a) Schematic of fingertip pressing status including (i) left side contact, (ii) right side contact, (iii) intermediate contact and (iv) rolling from left to right; (b) real-time output signals of the pressure sensor at different pressing angles; (c) feedback from the coin vibrators at different pressing angles with single vibrator running condition marked by grey and both vibrators running condition marked by pale yellow; (d) output signals from the bending sensor measure the stepped bending of the finger at an angle of 10 degrees each time up to 90 degrees; (e) response of the bending sensor under different bending methods; (f) various hand gestures labelled from ① to ⑧ used to test the bending sensor; (g) output signals corresponding to different hand gestures labelled from ② to ⑧; (h) demonstration of grasping a test tube; (i) feedback from coin vibrators during the grasping process; (j) real-time signal output during the grasp; and (k) snapshot of pressure and bending angles before and after grasping.

Based on the validation results, the bending sensors are sequentially integrated into the corresponding joints of the thumb and index finger, allowing our volunteers to wear the glove and perform seven different actions from a neutral hand position (Figure 6f①) to validate the feasibility of monitoring multi-joint coordinated movements (Figure 6f② to Figure 6f⑧). Each action lasts about five seconds. Specifically, action ① corresponds to the area with no signal fluctuations, action ② corresponds to only thumb I bending, action ③ corresponds to both thumbs I and II bending simultaneously, action ④ corresponds to only index finger I bending, action ⑤ corresponds to both index fingers I and II bending simultaneously, action ⑥ corresponds to index finger I and thumb I bending together, action ⑦ corresponds to all four sensors bending simultaneously, and action ⑧ corresponds to the thumb tightening toward the palm, similar to action ② but with a greater degree of bending in thumb II. Figure 6g shows the real-time signals captured from the four bending sensors, demonstrating that each bending sensor is activated by its respective joint and that the sensing signals fluctuate only when there is flexion or extension at the joint.

Furthermore, both the pressure sensors and bending sensors are integrated into the glove, demonstrating that the interactive glove can provide multi-dimensional force feedback and sense hand posture. Figure 6h–j illustrate the entire process of real-time force-posture signal monitoring (Figure 6j,k) as a volunteer wears the interactive glove to grasp a plastic test tube (Figure 6h). Again, on the feedback side, the pressure sensing unit is utilized to monitor the feedback force in real time, with the feedback intensities from the four coin vibrators shown in Figure 6i.

4. Discussion

In this work, we propose a facile design for a multi-dimensional pressure-sensing and feedback glove, aiming to address the problems of redundant system structure design and high complexity that may be faced when realizing multi-dimensional sensing and feedback. Elastic and hand-fitting gloves are chosen as the platform for integrating several minimalist functional units, including liquid metal microchannel-based strain and pressure sensors and vibration feedback actuators, and thus the flexible glove can effectively cover the different sizes of different users. The bending sensor located at the finger joints has a length of 2 cm, which means that there is a ± 1 cm tolerance from its effective sensing range, so the user does not need to align the joints with the center of the sensor, and hand postures can be accurately captured regardless of where the user's joint is located on the sensor. By projecting the flexion motion of individual joints into a virtual space or a manipulator, seamless tracking of hand posture is possible.

In addition, by evaluating the signal changes of the double symmetrically arranged pressure sensors at the tip of the finger, the glove is able to sense the direction and magnitude of the pressure and map it to the feedback unit in real time, and by adjusting the feedback strength of the vibration feedback actuators on both sides, multi-directional haptic feedback can be realized. This delicate feedback method can provide users with static and dynamic multi-dimensional haptic interaction information, which significantly enhances the user's sense of immersion and realism in the interactive environment. In addition, we also monitor the intensity of the vibration feedback in real time through the triboelectric sensing mechanism of the liquid metal sensor to ensure the stability and reliability of the interaction. On the other hand, due to the symmetrical distribution of two pressure sensors and two coin vibrators on each fingertip, the variation in finger size will not change the symmetry of these units but only increase the spacing between each one. To address this concern, with simple data calibration, two sensors are still performing the same capability of detecting multi-directional force by cooperatively analyzing two sensing signals. Similarly, two vibrators can still provide multi-directional haptic feedback, since they are still symmetrical, no matter whether the finger size is larger or smaller.

Experimental validation shows that the glove is able to effectively detect dynamic and static forces distributed in all directions of the fingertip, and it can accurately reconstruct hand movements to provide real-time multi-dimensional dynamic and static haptic feed-

back. The glove's simple modular design, low manufacturing cost, and multi-dimensional haptic information transfer capability show great potential for practical applications, especially for virtual reality, medical rehabilitation, and remote robot control, which require real-time interaction of multi-dimensional haptic information.

5. Conclusions

Current information transmission mainly relies on video- and audio-based communication. However, for teleoperation in industrial or medical applications, as well as remote or virtual social network, tactile communication becomes a key aspect to enhance the perception to interactive events in order to improve the efficiency of communication and reduce the potential risk caused by missing tactile information.

In conclusion, this paper proposes a cost-effective, multi-functional wearable HMI glove with an extremely simplified design to realize multi-dimensional pressure information sensing and feedback, and to capture the user's hand posture in real time, providing a new solution to enhance the user's HMI experience and a new reference for the future development of wearable HMI technology. Generally speaking, the gloves presented in this paper can be used in a variety of scenarios that require remote interaction, such as remote socialization, teleoperation, remote training, etc. Users can not only observe other users' hand postures through visual information but also sense the strength and direction of the pressure applied to their fingertips from a distance or in a virtual space through tactile information.

Supplementary Materials: The following supporting information can be downloaded at <https://www.mdpi.com/article/10.3390/act13110454/s1>, Text S1: Delays when processing the signals of both sensors; Figure S1: Comparison of the triboelectric output when the coin vibrator is placed in different positions; Figure S2: Cyclic test of the long-term operation of the pressure sensor and bending sensor; Figure S3: Characterization of the delays of both sensors when holding a beaker; Figure S4: Delay when processing the signals of both the pressure sensor and bending sensor.

Author Contributions: H.L.: Conceptualization, methodology, validation, investigation, visualization, writing—original draft, writing—review and editing. J.L.: Writing—original draft, editing, data curation, formal analysis and investigation. C.G.: Data curation, formal analysis, investigation. Y.W.: Data curation, formal analysis, investigation. T.C.: Conceptualization, methodology, validation, investigation, writing—review and editing, supervision, project administration. M.Z.: Conceptualization, methodology, validation, investigation, writing—review and editing, supervision, project administration. All authors have read and agreed to the published version of the manuscript.

Funding: This work was supported by the Natural Science Foundation of Jiangsu Province of China (Grant number BK20230480) and the National Natural Science Foundation of China (Grant numbers 62303340).

Data Availability Statement: Data are contained within the article.

Conflicts of Interest: The authors declare no conflicts of interest.

References

1. Kao, C.H.; Chen, C.C.; Jhu, W.Y.; Tsai, Y.T.; Chen, S.H.; Hsu, C.M.; Chen, C.Y. Novel Digital Glove Design for Virtual Reality Applications. *Microsyst. Technol.* **2018**, *24*, 4247–4266. [[CrossRef](#)]
2. Colella, N.; Bianchi, M.; Grioli, G.; Bicchi, A.; Catalano, M.G. A Novel Skin-Stretch Haptic Device for Intuitive Control of Robotic Prostheses and Avatars. *IEEE Robot. Autom. Lett.* **2019**, *4*, 1572–1579. [[CrossRef](#)]
3. Zhang, Z.; Wang, L.; Lee, C. Recent Advances in Artificial Intelligence Sensors. *Adv. Sens. Res.* **2023**, *2*, 2200072. [[CrossRef](#)]
4. Chen, T.; Dai, Z.; Liu, M.; Zhao, Y.; Ling, H.; Sun, L.; He, H.; Lee, C.; Zhu, M. 3D Multimodal Sensing and Feedback Finger Case for Immersive Dual-Way Interaction. *Adv. Mater. Technol.* **2024**, *9*, 2301681. [[CrossRef](#)]
5. Sun, Z.; Zhu, M.; Shan, X.; Lee, C. Augmented Tactile-Perception and Haptic-Feedback Rings as Human-Machine Interfaces Aiming for Immersive Interactions. *Nat. Commun.* **2022**, *13*, 5224. [[CrossRef](#)]
6. Ma, L.; Xia, T.; Yu, R.; Lei, X.; Yuan, J.; Li, X.; Cheng, G.J.; Liu, F. A 3D-printed, Sensitive, Stable, and Flexible Piezoresistive Sensor for Health Monitoring. *Adv. Eng. Mater.* **2021**, *23*, 2100379. [[CrossRef](#)]
7. Zheng, X.T.; Yang, Z.; Sutarlie, L.; Thangaveloo, M.; Yu, Y.; Salleh, N.A.B.M.; Chin, J.S.; Xiong, Z.; Becker, D.L.; Loh, X.J. Battery-Free and AI-Enabled Multiplexed Sensor Patches for Wound Monitoring. *Sci. Adv.* **2023**, *9*, eadg6670. [[CrossRef](#)]

8. Au, C.-Y.; Leow, S.Y.; Yi, C.; Ang, D.; Yeo, J.C.; Koh, M.J.A.; Bhagat, A.A.S. A Sensorised Glove to Detect Scratching for Patients with Atopic Dermatitis. *Sensors* **2023**, *23*, 9782. [[CrossRef](#)]
9. Li, G.; Liu, S.; Wang, L.; Zhu, R. Skin-Inspired Quadruple Tactile Sensors Integrated on a Robot Hand Enable Object Recognition. *Sci. Robot.* **2020**, *5*, eabc8134. [[CrossRef](#)]
10. Charalambides, A.; Bergbreiter, S. Tactile Sensors: Rapid Manufacturing of Mechanoreceptive Skins for Slip Detection in Robotic Grasping (Adv. Mater. Technol. 1/2017). *Adv. Mater. Technol.* **2017**, *2*. [[CrossRef](#)]
11. Boutry, C.M.; Negre, M.; Jorda, M.; Vardoulis, O.; Chortos, A.; Khatib, O.; Bao, Z. A Hierarchically Patterned, Bioinspired e-Skin Able to Detect the Direction of Applied Pressure for Robotics. *Sci. Robot.* **2018**, *3*, eaau6914. [[CrossRef](#)]
12. Hou, X.; Zhang, L.; Su, Y.; Gao, G.; Liu, Y.; Na, Z.; Xu, Q.; Ding, T.; Xiao, L.; Li, L. A Space Crawling Robotic Bio-Paw (SCRBP) Enabled by Triboelectric Sensors for Surface Identification. *Nano Energy* **2023**, *105*, 108013. [[CrossRef](#)]
13. Shih, B.; Shah, D.; Li, J.; Thuruthel, T.G.; Park, Y.-L.; Iida, F.; Bao, Z.; Kramer-Bottiglio, R.; Tolley, M.T. Electronic Skins and Machine Learning for Intelligent Soft Robots. *Sci. Robot.* **2020**, *5*, eaaz9239. [[CrossRef](#)] [[PubMed](#)]
14. Yao, K.; Zhou, J.; Huang, Q.; Wu, M.; Yiu, C.K.; Li, J.; Huang, X.; Li, D.; Su, J.; Hou, S.; et al. Encoding of Tactile Information in Hand via Skin-Integrated Wireless Haptic Interface. *Nat. Mach. Intell.* **2022**, *4*, 893–903. [[CrossRef](#)]
15. Huang, Y.; Zhou, J.; Ke, P.; Guo, X.; Yiu, C.K.; Yao, K.; Cai, S.; Li, D.; Zhou, Y.; Li, J. A Skin-Integrated Multimodal Haptic Interface for Immersive Tactile Feedback. *Nat. Electron.* **2023**, *6*, 1020–1031. [[CrossRef](#)]
16. Guo, H.; Pu, X.; Chen, J.; Meng, Y.; Yeh, M.-H.; Liu, G.; Tang, Q.; Chen, B.; Liu, D.; Qi, S. A Highly Sensitive, Self-Powered Triboelectric Auditory Sensor for Social Robotics and Hearing Aids. *Sci. Robot.* **2018**, *3*, eaat2516. [[CrossRef](#)] [[PubMed](#)]
17. Chen, Y.; Lei, H.; Gao, Z.; Liu, J.; Zhang, F.; Wen, Z.; Sun, X. Energy Autonomous Electronic Skin with Direct Temperature-Pressure Perception. *Nano Energy* **2022**, *98*, 107273. [[CrossRef](#)]
18. Gul, O.; Kim, K.; Gu, J.; Choi, J.; Del Orbe Henriquez, D.; Ahn, J.; Park, I. Sensitivity-Controllable Liquid-Metal-Based Pressure Sensor for Wearable Applications. *ACS Appl. Electron. Mater.* **2021**, *3*, 4027–4036. [[CrossRef](#)]
19. Sun, Z.; Zhang, S.; Lee, C. A Skin-like Multimodal Haptic Interface. *Nat. Electron.* **2023**, *6*, 941–942. [[CrossRef](#)]
20. Oh, J.; Kim, S.; Lee, S.; Jeong, S.; Ko, S.H.; Bae, J. A Liquid Metal Based Multimodal Sensor and Haptic Feedback Device for Thermal and Tactile Sensation Generation in Virtual Reality. *Adv. Funct. Mater.* **2021**, *31*, 2007772. [[CrossRef](#)]
21. Yu, R.; Xia, T.; Wu, B.; Yuan, J.; Ma, L.; Cheng, G.J.; Liu, F. Highly Sensitive Flexible Piezoresistive Sensor with 3D Conductive Network. *ACS Appl. Mater. Interfaces* **2020**, *12*, 35291–35299. [[CrossRef](#)] [[PubMed](#)]
22. Mengüç, Y.; Park, Y.-L.; Pei, H.; Vogt, D.; Aubin, P.M.; Winchell, E.; Fluke, L.; Stirling, L.; Wood, R.J.; Walsh, C.J. Wearable Soft Sensing Suit for Human Gait Measurement. *Int. J. Rob. Res.* **2014**, *33*, 1748–1764. [[CrossRef](#)]
23. Tehrani, F.; Teymourian, H.; Wuerstle, B.; Kavner, J.; Patel, R.; Furnidge, A.; Aghavali, R.; Hosseini-Toudeshki, H.; Brown, C.; Zhang, F. An Integrated Wearable Microneedle Array for the Continuous Monitoring of Multiple Biomarkers in Interstitial Fluid. *Nat. Biomed. Eng.* **2022**, *6*, 1214–1224. [[CrossRef](#)]
24. Yang, Y.; Guo, X.; Zhu, M.; Sun, Z.; Zhang, Z.; He, T.; Lee, C. Triboelectric Nanogenerator Enabled Wearable Sensors and Electronics for Sustainable Internet of Things Integrated Green Earth. *Adv. Energy Mater.* **2023**, *13*, 2203040. [[CrossRef](#)]
25. Zhang, Q.; Jin, T.; Cai, J.; Xu, L.; He, T.; Wang, T.; Tian, Y.; Li, L.; Peng, Y.; Lee, C. Wearable Triboelectric Sensors Enabled Gait Analysis and Waist Motion Capture for IoT-based Smart Healthcare Applications. *Adv. Sci.* **2022**, *9*, 2103694. [[CrossRef](#)]
26. Shin, S.; Yoon, H.U.; Yoo, B. Hand Gesture Recognition Using EGaIn-Silicone Soft Sensors. *Sensors* **2021**, *21*, 3204. [[CrossRef](#)]
27. Zhu, M.; Sun, Z.; Lee, C. Soft Modular Glove with Multimodal Sensing and Augmented Haptic Feedback Enabled by Materials' Multifunctionalities. *ACS Nano* **2022**, *16*, 14097–14110. [[CrossRef](#)]
28. Shen, Z.; Yi, J.; Li, X.; Lo, M.H.P.; Chen, M.Z.Q.; Hu, Y.; Wang, Z. A Soft Stretchable Bending Sensor and Data Glove Applications. *Robot. Biomim.* **2016**, *3*, 22. [[CrossRef](#)]
29. Kim, K.-H.; Hong, S.K.; Jang, N.-S.; Ha, S.-H.; Lee, H.W.; Kim, J.-M. Wearable Resistive Pressure Sensor Based on Highly Flexible Carbon Composite Conductors with Irregular Surface Morphology. *ACS Appl. Mater. Interfaces* **2017**, *9*, 17499–17507. [[CrossRef](#)]
30. González, C.; Solanes, J.E.; Muñoz, A.; Gracia, L.; Girbés-Juan, V.; Tornero, J. Advanced Teleoperation and Control System for Industrial Robots Based on Augmented Virtuality and Haptic Feedback. *J. Manuf. Syst.* **2021**, *59*, 283–298. [[CrossRef](#)]
31. Lee, E.-H.; Kim, S.-H.; Yun, K.-S. Three-Axis Pneumatic Haptic Display for the Mechanical and Thermal Stimulation of a Human Finger Pad. *Actuators* **2021**, *10*, 60. [[CrossRef](#)]
32. Li, B.; Shi, Y.; Hu, H.; Fontecchio, A.; Visell, Y. Assemblies of Microfluidic Channels and Micropillars Facilitate Sensitive and Compliant Tactile Sensing. *IEEE Sens. J.* **2016**, *16*, 8908–8915. [[CrossRef](#)]
33. Park, Y.-L.; Chen, B.-R.; Wood, R.J. Design and Fabrication of Soft Artificial Skin Using Embedded Microchannels and Liquid Conductors. *IEEE Sens. J.* **2012**, *12*, 2711–2718. [[CrossRef](#)]
34. Hammond, F.L.; Mengüç, Y.; Wood, R.J. Toward a Modular Soft Sensor-Embedded Glove for Human Hand Motion and Tactile Pressure Measurement. In Proceedings of the 2014 IEEE/RSJ International Conference on Intelligent Robots and Systems, Chicago, IL, USA, 14–18 September 2014; IEEE: Piscataway, NJ, USA, 2014; pp. 4000–4007.
35. Kim, S.; Oh, J.; Jeong, D.; Bae, J. Direct Wiring of Eutectic Gallium–Indium to a Metal Electrode for Soft Sensor Systems. *ACS Appl. Mater. Interfaces* **2019**, *11*, 20557–20565. [[CrossRef](#)]
36. Lee, W.W.; Tan, Y.J.; Yao, H.; Li, S.; See, H.H.; Hon, M.; Ng, K.A.; Xiong, B.; Ho, J.S.; Tee, B.C.K. A Neuro-Inspired Artificial Peripheral Nervous System for Scalable Electronic Skins. *Sci. Robot.* **2019**, *4*, eaax2198. [[CrossRef](#)]

37. Singh, R.; Mozaffari, S.; Akhshik, M.; Ahamed, M.J.; Rondeau-Gagné, S.; Alirezaee, S. Human–Robot Interaction Using Learning from Demonstrations and a Wearable Glove with Multiple Sensors. *Sensors* **2023**, *23*, 9780. [[CrossRef](#)]
38. Boley, J.W.; White, E.L.; Chiu, G.T.; Kramer, R.K. Direct Writing of Gallium-indium Alloy for Stretchable Electronics. *Adv. Funct. Mater.* **2014**, *24*, 3501–3507. [[CrossRef](#)]
39. Kim, S.; Oh, J.; Jeong, D.; Park, W.; Bae, J. Consistent and Reproducible Direct Ink Writing of Eutectic Gallium–Indium for High-Quality Soft Sensors. *Soft Robot.* **2018**, *5*, 601–612. [[CrossRef](#)]
40. Gao, Y.; Ota, H.; Schaler, E.W.; Chen, K.; Zhao, A.; Gao, W.; Fahad, H.M.; Leng, Y.; Zheng, A.; Xiong, F.; et al. Wearable Microfluidic Diaphragm Pressure Sensor for Health and Tactile Touch Monitoring. *Adv. Mater.* **2017**, *29*, 1701985. [[CrossRef](#)]
41. Kim, D.; Kwon, J.; Han, S.; Park, Y.-L.; Jo, S. Deep Full-Body Motion Network for a Soft Wearable Motion Sensing Suit. *IEEE/ASME Trans. Mechatron.* **2018**, *24*, 56–66. [[CrossRef](#)]
42. Liu, M.; Dai, Z.; Zhao, Y.; Ling, H.; Sun, L.; Lee, C.; Zhu, M.; Chen, T. Tactile Sensing and Rendering Patch with Dynamic and Static Sensing and Haptic Feedback for Immersive Communication. *ACS Appl. Mater. Interfaces* **2024**, *16*, 53207–53219. [[CrossRef](#)] [[PubMed](#)]
43. Pan, H.; Chen, G.; Chen, Y.; Di Carlo, A.; Mayer, M.A.; Shen, S.; Chen, C.; Li, W.; Subramaniam, S.; Huang, H. Biodegradable Cotton Fiber-Based Piezoresistive Textiles for Wearable Biomonitoring. *Biosens. Bioelectron.* **2023**, *222*, 114999. [[CrossRef](#)] [[PubMed](#)]
44. Ma, Y.; Liu, N.; Li, L.; Hu, X.; Zou, Z.; Wang, J.; Luo, S.; Gao, Y. A Highly Flexible and Sensitive Piezoresistive Sensor Based on MXene with Greatly Changed Interlayer Distances. *Nat. Commun.* **2017**, *8*, 1207. [[CrossRef](#)]
45. JK O’Neill, S.; Gong, H.; Matsuhisa, N.; Chen, S.; Moon, H.; Wu, H.; Chen, X.; Chen, X.; Bao, Z. A Carbon Flower Based Flexible Pressure Sensor Made from Large-area Coating. *Adv. Mater. Interfaces* **2020**, *7*, 2000875. [[CrossRef](#)]
46. Tao, L.-Q.; Zhang, K.-N.; Tian, H.; Liu, Y.; Wang, D.-Y.; Chen, Y.-Q.; Yang, Y.; Ren, T.-L. Graphene-Paper Pressure Sensor for Detecting Human Motions. *ACS Nano* **2017**, *11*, 8790–8795. [[CrossRef](#)]
47. Araromi, O.A.; Graule, M.A.; Dorsey, K.L.; Castellanos, S.; Foster, J.R.; Hsu, W.-H.; Passy, A.E.; Vlassak, J.J.; Weaver, J.C.; Walsh, C.J. Ultra-Sensitive and Resilient Compliant Strain Gauges for Soft Machines. *Nature* **2020**, *587*, 219–224. [[CrossRef](#)] [[PubMed](#)]
48. Lee, S.; Wang, H.; Wang, J.; Shi, Q.; Yen, S.-C.; Thakor, N.V.; Lee, C. Battery-Free Neuromodulator for Peripheral Nerve Direct Stimulation. *Nano Energy* **2018**, *50*, 148–158. [[CrossRef](#)]
49. Jiang, C.; Li, X.; Yao, Y.; Lan, L.; Shao, Y.; Zhao, F.; Ying, Y.; Ping, J. A Multifunctional and Highly Flexible Triboelectric Nanogenerator Based on MXene-Enabled Porous Film Integrated with Laser-Induced Graphene Electrode. *Nano Energy* **2019**, *66*, 104121. [[CrossRef](#)]

Disclaimer/Publisher’s Note: The statements, opinions and data contained in all publications are solely those of the individual author(s) and contributor(s) and not of MDPI and/or the editor(s). MDPI and/or the editor(s) disclaim responsibility for any injury to people or property resulting from any ideas, methods, instructions or products referred to in the content.